Cryogenic thermal emittance measurements on small-diameter stainless steel tubing

Amir E. Jahromi*, James G. Tuttle, Edgar R. Canavan

NASA Goddard Space Flight Center, Code 552, Greenbelt MD 20771, U.S.A.

*Corresponding author
amir.e.jahromi@nasa.gov

Abstract. The Mid Infrared Instrument aboard the James Webb Space Telescope includes a mechanical cryocooler which cools its detectors to their 6 K operating temperature. The refrigerant flows through several meters of ~2 mm diameter 304L stainless steel tubing, with some sections gold plated, and some not, which are exposed to a varied thermal environment. An issue of water freezing onto the tube surfaces is mitigated by periodically running a warm gas through the lines to sublimate the frozen water. To model the effect of this process on nearby instruments, an accurate measure of the tube emittance is needed. Previously we reported the absorptance of the gold plated stainless steel tubing as a function of source temperature (i.e. its environment). In this work the thermal emittance of the uncoated tubing is measured as a function of its temperature between 100 and 280 K. These values lead to an accurate prediction of the impact of thermally recycling the system. We report the technique and present the results.

1. Introduction

The Mid Infrared Instrument (MIRI) aboard the James Webb Space Telescope (JWST) includes a Joule-Thomson (JT) cooler that maintains its detectors at an operating temperature of 6 K upon expansion of helium gas, after it is precooled to 18 K by a pulse-tube cryocooler. The 18 K helium will flow to the JT valve through several meters of small-diameter gold plated, and uncoated stainless steel tubing. Different sections of these tubes are exposed to different environments within the instrument with complex view factors. The gold plated sections are exposed to environments where radiation heat leak onto the tubing must be minimized to ensure MIRI cooler meets mission requirements, while uncoated sections are exposed to very well thermally-isolated components where radiation heat leak onto the tubing is of minimal concern during normal operation. We previously reported the absorptance of the gold plated tubing as a function of source temperature [1]. These measured values were found to be below a certain expected maximum value at 18 K operating temperature, the temperature at which the tube absorbs heat. This was reassuring to the mission.

A study conducted by the JWST thermal team predicts that very small amounts of water will freeze on the surfaces of the MIRI cooler line's tubing. It is predicted that this effect will gradually increase the gold plated tube's absorptance as more water freezes onto their surfaces over time. This undesirable effect will lead to a higher radiation heat leak from the surrounding environment onto the tube, and in turn, the refrigerant flowing through those sections. Therefore the MIRI cooler will need to be thermally recycled (warmed up) as needed, in order to sublimate frozen water from such surfaces by flowing

sufficiently warm gas (~200K) through the affected sections. The length of time that the lines should be held at this elevated temperature is currently being assessed by the project. While warm, the uncoated sections will radiate heat onto the thermally-isolated components surrounding them. The longer the recycling time, the more heat leaks into the thermally-isolated components due to radiation, the longer it will take to cool these components back down to their original temperature before resuming MIRI cooler's normal operation. To understand the impact of this process, it was desirable to directly measure the thermal radiation power emitted by this uncoated stainless steel tubing per unit length as a function of its surface temperature. We describe a test that was carried out by suspending a length of the tube inside a blackbody cavity and measuring the power it emitted as a function of its surface temperature.

1. Theory

The theory related to predicting absorptivity values was presented in a previous publication by Tuttle et. al. [1]. Our intention is to provide a refresher on pertinent theory, specifically presenting a model that predicts emissivity of metals as a function of their temperature.

When an opaque body does not reflect any radiation it is called a perfect absorber or a blackbody (a rather theoretical concept). Blackbody objects have the following three properties: 1) they absorb all of the radiation that is incident upon them, regardless of direction or wavelength 2) they emit radiation in all directions (diffuse emitter) and 3) they emit the maximum possible amount of radiation at a given temperature and wavelength. When an object, such as the uncoated stainless steel tubing studied in this work, is suspended inside an isothermal blackbody cavity it emits electromagnetic waves at different frequencies, and random directions. The ratio of this emission at each frequency and direction, to that of a blackbody at the same temperature is referred to as spectral, directional emittance. Once this value is integrated over the entire spectrum for a specific direction it is called total emittance. And once this value is integrated over all directions, it is called total hemispherical emittance defined as:

$$\varepsilon(T_s) = \frac{E(T_s)}{E_b(T_s)} \tag{1}$$

where T_s is the object's own temperature, and E is the emissive power where subscript b denotes blackbody. In practice, this value is used as a key parameter in predicting radiative heat exchange between surfaces. Note that in order to stay consistent with NIST's convention we have reserved radiative properties ending in "-ivity" (i.e. emissivity) for theoretical and optically smooth surfaces, while those ending in "-ance" (i.e. emittance) are reserved for real surfaces.

The radiative thermal power leaving the suspended object depends on its surface area A_s, its emittance ε, which is a function of its own temperature T_s as defined by the following equation:

$$\dot{Q}_{s\to cavity} = \varepsilon(T_s)\, A_s\, \sigma\, T_s^4 \tag{2}$$

where $\sigma = 5.67 \times 10^{-8}$ ($W/m^2\text{-}K^4$) is the Stefan-Boltzmann constant. Note that unlike absorptivity, the emissivity of a material depends on its temperature, but not on its surroundings.

The Hagen-Rubens relation predicts that the spectral normal emittance of a metal should be proportional to the square root of the product of its temperature and DC electrical resistivity. Since the DC electrical resistivity is approximately proportional to temperature, the spectral emittance should be proportional to the temperature for long enough wavelengths. This approach should also hold true for the spectral, hemispherical emissivity as it has been shown to be true for many metals through various experiments [2]. In pursuit of finding a relationship between emissivity and temperature Parker and Abbott [3] were able to analytically integrate the spectral, hemispherical emissivity for a metal using Fresnel's relations and applying Kirchhoff's law and express it in terms of the metal's surface temperature in (K), and its DC electrical resistivity in (Ω-cm):

$$\varepsilon(T_s) = 0.766\sqrt{T_s\,\rho_{dc}} - \left[0.309 - 0.0889\ln(T_s\,\rho_{dc})\right] T_s\,\rho_{dc} - 0.0175\,T_s\,\rho_{dc}\sqrt{T_s\,\rho_{dc}} \tag{3}$$

Eq (3) is valid as long as the surface temperature is relatively low (such as those used in this work) so that only long wavelengths are of importance for which the Hagen-Rubens relation provides reasonable results.

As presented later in this work, we verified the integrity of our experimental setup by measuring the absorptance values of the uncoated stainless steel tubing as a function of the tube temperature (absorber) and the blackbody cavity temperature (emitter) by repeating methods discussed in our previous work [1]. The total hemispheric absorptivity of a metal is approximated according to:

$$\alpha(T_b) \approx B\,\alpha_{\perp} \quad where \quad \alpha_{\perp} = 0.576\sqrt{\rho_{dc}\,T_b} - 0.124\,\rho_{dc}\,T_b \tag{4}$$

where the constant B is approximately 1.3 for very reflective surfaces. Here ρ_{dc} is the absorbing surface resistivity in (Ω-cm), which depends on the absorber's temperature, and T_b is the blackbody source temperature. We noted that it would not be surprising if Eq. (4) under-predicts the absorptance of a surface when ρ_{dc} is assumed to be the bulk resistivity due to reasons discussed in the previous work. However, it is still expected for the measured absorptance values to follow a square root of source temperature dependence, as seen later in this work.

2. Experimental setup

Our goal was to suspend a sample length of the uncoated AISI 304L stainless steel MIRI cooler tube inside a blackbody cavity, control the tube at various discrete temperatures, and measure the radiation power it emitted to the cavity walls. To accomplish this the same apparatus previously used for measuring the absorptance of a gold-plated stainless steel tubing was utilized. The apparatus consists of a simulated environment and a sample sub-assembly.

The simulated environment was made out of a thick-walled 10 cm x 10 cm x 30 cm rectangular aluminum box, with black-painted aluminum honeycomb epoxied to the insides and the top/bottom plates as shown in **Figure 1**. The "box" was mounted above a lab cryostat's cold plate on thermally insulating stand-offs, with engineered heat straps thermally connecting the box bottom to the cold plate. Thermometers and heaters at the box ends allowed it to be controlled in an isothermal condition at selected temperatures.

The tubing sub-assembly consisted of a length of uncoated stainless steel tubing with an outer and inner diameters of 1.96 mm and 1.29 mm, respectively. A copper wire ran through the center of the tube, occupying approximately 60% of the internal cross sectional area. This wire, which extended a few mm out of each end of the tube, was potted with degassed Stycast 2850 epoxy. It minimized thermal gradients along the length of the tubing sub-assembly. A very thin sample heater wire, only 0.05 mm in diameter, was imbedded in the stycast epoxy. This long heater wire was folded on itself and made multiple longitudinal passes inside the tube. This high electrical resistivity wire was chosen specifically

Figure 1. Simulation environment: This thick-walled rectangular aluminum box with black-painted honeycomb epoxied to the insides provides an environment with an emissivity and absorptivity close to 1.0.

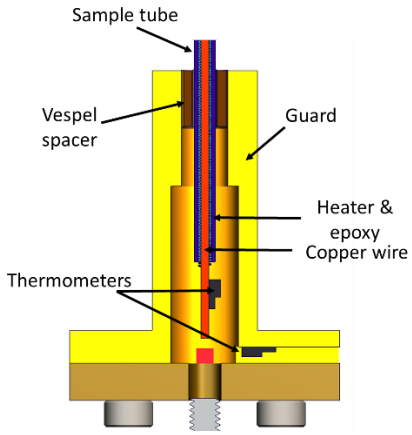

Figure 2. Each guard consists of a copper sleeve that covers an end of the stainless steel tubing and is thermally connected to it via a Vespel spacer ring in the annular void between the tube and the sleeve. The guards ensure that the sample's ends have no radiative heat exchange with the box .

to enable a high heater resistance, which is necessary to minimize the uncertainty in determining the heater power applied to the sample during the test. Thermally engineered current and voltage leads, made of insulated 0.12 mm diameter stainless steel, were soldered to each end of the heater wire. These leads were thermally attached to the copper wire external to each end of the tube. A tiny sample thermometer was bonded to the copper wire, external to one end of the tube as shown in **Figure 2**.

Each end of the tube-heater sub-assembly was positioned inside a cylindrical copper "guard," as shown in **Figure 2**. A ring of Vespel was epoxied in place in the annular space between the tubing and the copper sleeve. The Vespel provided a fixed thermally-conductive connection between the sample tube and each guard, while ensuring that no thermal radiation was exchanged between the inside of the guard and the box. The ends of the sample tube, the extending copper wires, the sample thermometer, and the heater and thermometer leads were all located inside the guard volume. This was important, since these objects could not be allowed to have radiative heat exchange with the box. The resulting geometry allowed only radiative heat exchange between the smooth surface of the sample and the box. All heat exchange between the sample and the guards occurred inside the guards, independent of the box temperature.

Each guard was supported so that it passed through a hole in one of the box's ends, with its inner face flush with the inner extent of the painted honeycomb. A flange on the back of each guard served as a baffle to keep thermal radiation from entering or leaving the box around the guard. The bottom guard was stood off from the cold plate via a stainless steel threaded rod. Thermal straps were added to the guards to allow for thermal communication between them and the cold plate. A copper bus bar was needed to emulate a cold temperature environment for the top guard due to its positional isolation relative to the cold plate. The entire assembly is shown in **Figure 3**.

Through initial measurements we noticed indications of a temperature offset between the sample thermometer and the tube's outer surface. This issue was mitigated later by modifying the experiment to accommodate two pairs of electrical leads carefully silver epoxied to the tube, near its ends. These leads were actually bonded to the tube inside side-drilled holes through the guards and the Vespel insulators. Note that the electrical isolation of the tube from the guards was verified prior to implementing this technique. This allowed for real-time measurement of the electrical resistance of the tube, which was directly tied to the temperature of the tube. Monitoring the tube's resistance allowed the tube's surface temperature to be kept constant as the test conditions were changed. More on this to be followed in the measurement technique section.

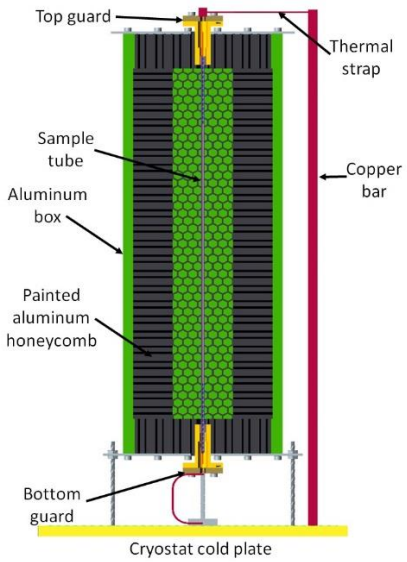

Figure 3. The entire assembly consists of the box and sample sub-assembly. The whole assembly was used to measure the radiative properties of the tubing reported in this document.

3. Measurement technique

The project was primarily concerned with the emittance of the tube at 200 K. However, we measured the power emitted by the sample tube at discrete temperatures between 100 and 280 K. The pressure in the vacuum chamber was verified to be in the 1 x 10^{-8} Torr range. Thus, the effects of convection heat transfer and residual gas conduction were negligible.

We began our measurement by controlling the temperatures of the sample, guards, and the box to the same value (e.g. 200 K) to create an isothermal environment. In order to ensure a positive power control of the sample tube we ever-so-slightly dropped the guard temperatures (e.g. by 2 mK) relative to the sample and noted the measured sample control power as our "zero radiated power" measurement (e.g. 20 microwatts). This resulted in no thermal radiative communication between the sample and the box, but a small amount of "zero" heat conduction from the sample to the guards. We also took note of the electrical resistance of the tube under these conditions. This was an important step, because with no heat radiating from the sample, its surface temperature equalled that measured by the sample thermometer. Since the electrical resistance of the tubing is a function of temperature, we effectively created a "thermometer" out of the entire stainless steel tubing. We calibrated this thermometer by varying its temperature prior to the emittance measurements and found a sensitivity of ~140 μohm/K for the tube between 100 and 280 K. Note that we were able to resolve 1 micro-ohm with great stability.

The experiment proceeded by dropping the temperature of the box to its minimum attainable temperature while holding the guards and the sample thermometer at the initial "isothermal" temperature value. This minimum box temperature, which was close to the 3 K cold plate temperature, was so much colder than the sample that its exact value had no appreciable effect on the data analysis.

Dropping the temperature of the box required the sample heater power to rise in order to compensate for the "lost radiative power" while maintaining the sample temperature. The heater power was conducted radially outward through the epoxy and the stainless steel tubing to its surface, from which it radiated to the box. The resulting radial temperature drop caused the stainless steel tubing to cool below the temperature of the sample sensor, as indicated by a drop in the tubing resistance. A simple calculation showed that this amount of heat conducted radially through the stainless steel thickness would produce a negligible radial temperature drop in the stainless steel. Thus, the stainless steel could be considered radially isothermal, and the temperature indicated by its resistance was that of the radiating surface. The radial temperature drop must have been in the epoxy or in the surface interface between the epoxy and stainless tubing.

At this point we raised the sample control setpoint until the tubing resistance returned to the exact value we had measured before dropping the box temperature. Now, with the sample surface back at its original temperature, we could compare the measured heat with its "zero-radiation" value in the isothermal state. The difference between these two heat values was the radiated power at this surface temperature.

The integrity of the experiment was supported by making an absorptance measurement similar to our earlier characterization of a gold-plated sample in this same apparatus. For this measurement we originally set the temperature of the entire assembly to a relatively low temperature at 50 K. We imposed a temperature gradient between the guards and the sample by controlling the temperature of the guards a few Kelvin below that of the sample. This enabled us to establish a "zero-radiation" sample power value to be used as a reference. Then we varied the box temperature while holding all other variables constant resulting in a drop of sample power as the box temperature was raised. This is because a drop in sample power is compensated by a rise in the radiative power from the box onto the sample. We recorded the sample power at various box temperatures and subtracted them from the "zero-radiation" measurement to arrive at the power absorbed by the sample. According to theory and physical principles the absorptivity of a sample at constant temperature must rise as the square root of radiation source temperature, and in fact we got an almost exact agreement between our measurement and theory. Our data analysis shows this expected behavior in subsequent sections.

4. Data analysis

The objective of this section is to present the data analysis used to arrive at emittance, electrical resistivity, and limited absorptance values found for the uncoated AISI 304L Stainless Steel tubing used in this experiment.

The analysis begins by revisiting the heat transfer rate due to radiation between the sample tube and its surroundings (interiors of the cavity):

$$\dot{Q}_{s\to b} = \frac{E_{b,s} - E_{b,b}}{R_s + R_{s\to b} + R_b} \tag{5}$$

where E is the blackbody emissive power ($\sigma \cdot T^4$) , R is the surface resistances and subscripts s and b denote sample and box respectively. The surface resistances are defined as:

$$R_s = \frac{1-\varepsilon_s}{\varepsilon_s} \quad \& \quad R_b = \frac{1-\varepsilon_b}{\varepsilon_b} = 0 \quad \text{since} \quad \varepsilon_b \approx 1 \tag{6}$$

where ε is the emissivity. $R_{s\to b}$ is the space resistance defined by:

$$R_{s\to b} = \frac{1}{A_s\, F_{s\to b}} = \frac{1}{A_s} \ \text{ since } \ F_{s\to b} \approx 1 \tag{7}$$

where $F_{s\to b}$ is the view factor from the sample to the box and A_s is the effective surface area of the sample exposed to the surroundings. Combining Eq. (6) and (7) into Eq. (5) yields:

$$\dot{Q}_{s\to b} = \sigma\, A_s\, \varepsilon_s \left(T_s^4 - T_b^4\right) \tag{8}$$

The effective surface area of the tubing is calculated based on a 1.96 mm diameter and 26 cm exposed length. We note that the length of tubing, copper wire, sensors, and attachments beyond the exposed length were shielded, as they occupied the space internal to each guard. Hence, there was no radiative heat exchange between the extremities and the box. The "zero-radiation" power for each set of measurement is subtracted from the measured power in order to obtain the true radiative power. At this point the box, sample temperature, sample heater power, and effective surface area are known, so it is possible to calculate an emittance for each measured sample temperature. Similarly the electrical resistivity of the material used in the tubing is found by multiplying the measured resistance by the cross sectional area of the tube and dividing it by the length between the voltage taps.

The theoretical values of emissivity found through Eq. (3), using the measured electrical resistivity, and experimental values found through this work differ by as much as 30%. We believe that this

mismatch is attributed to the fact that Eq. (3) assumes a perfectly smooth surface, whereas real surfaces similar to that used as the sample in this work assume a surface roughness due to manufacturing and post-handling (surfaces with repeatable grooved finish, i.e. V-grooves, circular grooves, etc.). Wen et. al. [4] presents a method to account for surface roughness when estimating emittance values of metals. Within the geometric region, where the ratio of surface roughness ξ, to the wavelength λ, exceeds unity, the emittance of a real surface is adjusted based on:

$$\varepsilon_r = \left[1 + \left(\frac{1}{\varepsilon_{th}} - 1\right)\chi\right]^{-1} \tag{9}$$

where the subscripts *r* and *th* denote real, and theoretical respectively and χ is the roughness factor defined as:

$$\chi = \left(1 + 1.25\,\pi^2\, n^2\, R_a^2\right)^{-1} \tag{10}$$

where *n* is the number of intersections of the surface profile with the mean, per unit length of the mean line, and R_a is the mean arithmetic deviation of the profile as commonly found in published material property tables. Unfortunately the roughness characteristics of the sample were not available to us at this time. Thus we made an attempt to find a combined value of R_a and *n* by matching our measured emittance value with the predicted emittance at 100 K, using our measured electrical resistivity values (for example values of R_a and *n* of 1.6 micron and 0.1 micron^{-1} respectively are found reasonable for unprocessed extruded metals [5]). We then used these values to predict the emittance at higher temperatures. The results are tabulated in **Table 1** and graphically shown in **Figure** 4. As it can be seen, the predicted and measured values agree well at higher temperatures.

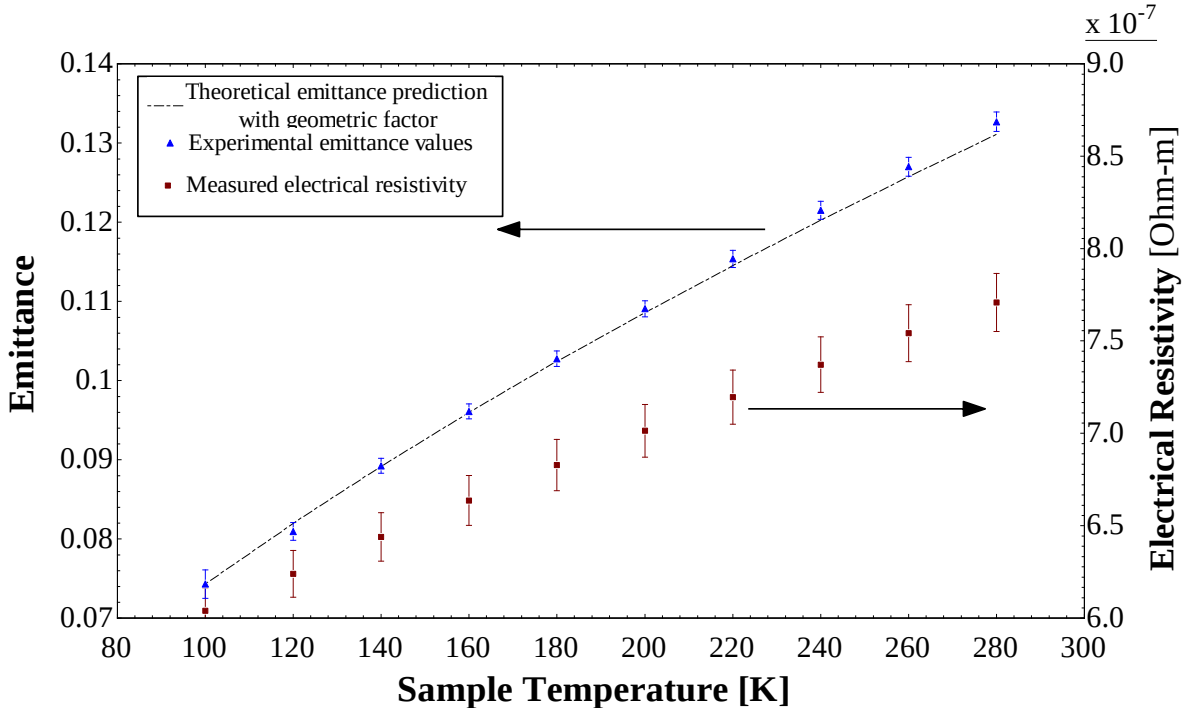

Figure 4. The measured emittance of the sample. The dashed line represent the emissivity predicted by theory after incorporating adjustment due to surface roughness.

Sample T (K)	Emitted power/length (W/m)	Emittance	Electrical Resistivity (Ω-cm)
100	2.593×10^{-3}	0.07429	6.039×10^{-5}
120	5.857×10^{-3}	0.08093	6.239×10^{-5}
140	1.196×10^{-2}	0.08923	6.439×10^{-5}
160	2.198×10^{-2}	0.09609	6.636×10^{-5}
180	3.765×10^{-2}	0.10275	6.828×10^{-5}
200	6.091×10^{-2}	0.10906	7.013×10^{-5}
220	9.433×10^{-2}	0.11537	7.195×10^{-5}
240	1.407×10^{-1}	0.12151	7.371×10^{-5}
260	2.026×10^{-1}	0.12700	7.542×10^{-5}
280	2.847×10^{-1}	0.13268	7.707×10^{-5}

Table 1. Emittance, emitted power per unit length, and electrical resistivity data for the uncoated stainless steel tubing

A limited number of points were selected to measure the absorptance of the sample to ensure integrity of the apparatus by comparison with theory presented in our previous work [1]. The absorptivity of the sample must follow as the square root of the cavity's temperature as one holds the sample temperature constant. Fitting a power law (absorptance = AT^b) through the data revealed a power, b, of 0.4998, which is spectacularly close to the 0.5 predicted by theory. Results of the absorptance values are tabulated in **Table 2**.

Sample T (K)	Box T (K)	Absorbed power/length (W/m)	Absorptance
50	150	4.060×10^{-3}	0.08934
50	200	14.94×10^{-3}	0.10312
50	220	22.98×10^{-3}	0.10821

Table 2. Limited absorptance data for the uncoated stainless steel tubing

5. Conclusion

In this work we presented the results of our emittance measurement of a stainless steel tubing, sample representative of the one used in the MIRI cooler system aboard the JWST, compared to theory, and discussed the data analysis used to arrive at the results. We verified the integrity of the apparatus and the experiment through a separate add-on measurement and confirmed that the entire system functioned as planned.

References

[1] Tuttle JG, Jahromi AE, Canavan ER, and DiPirro MJ. "Cryogenic thermal absorptance measurements on small-diameter stainless steel tubing." Cryogenics 74 (2016), p. 166-171.

[2] Modest MF. Radiative Heat Transfer. Amsterdam: Academic Press, 2003.

[3] Abbot GL, and Parker WJ. "Theoretical and experimental studies of the total emittance of metals", in Symposium on Thermal Radiation of Solids, S. Katzoff, ed., NASA SP-55 (1965), p. 11-28.

[4] Wen C, and Mudawar I. "Modeling the effects of surface roughness on the emissivity of aluminum alloys", International Journal of Heat and Mass Transfer, Volume 49, Issue 23, (2006), p. 4279-4289

[5] Hoffman PJ, Hopewell ES, Janes B, Sharp Jr KM. Precision machining technology. Cengage Learning, 2012.

Acknowledgements

This work was supported by NASA's Cosmic Origins program.